

---

# Comprehensive Investigation of Crystallographic Architectures, Electronic Bandgap Characteristics, and Anisotropic Mechanical Properties in Ternary Tellurides $KAlTe_2$ and $KInTe_2$ Employing WIEN2k and CASTEP Computational Paradigms

---

[Zahid Ullah](#)<sup>\*</sup>, Muhammad Amir Khan, Sabahat Gul

Posted Date: 7 January 2025

doi: 10.20944/preprints202501.0496.v1

Keywords: DDT; WIEN2k



Preprints.org is a free multidisciplinary platform providing preprint service that is dedicated to making early versions of research outputs permanently available and citable. Preprints posted at Preprints.org appear in Web of Science, Crossref, Google Scholar, Scilit, Europe PMC.

Copyright: This open access article is published under a Creative Commons CC BY 4.0 license, which permit the free download, distribution, and reuse, provided that the author and preprint are cited in any reuse.

Article

# Comprehensive Investigation of Crystallographic Architectures, Electronic Bandgap Characteristics, and Anisotropic Mechanical Properties in Ternary Tellurides $KAlTe_2$ and $KInTe_2$ Employing WIEN2k and CASTEP Computational Paradigms

Zahid Ullah <sup>1,2,\*</sup>, Muhammad Amir Khan <sup>1,\*</sup> and Sabahat Gul <sup>1,2</sup>

<sup>1</sup> Faculty of Physical and Numerical Sciences, Qurtuba University of Science and Information Technology Peshawar/D.I Khan Pakistan.

<sup>2</sup> Physics Department Islamia College University Peshawar Pakistan.

\* Correspondence: zuzohaad@gmail.com (Z.U.); makphy83@gmail.com (M.A.K.)

**Abstract:** A first-principles study was performed on the anisotropic ternary compounds  $KAlTe_2$  and  $KInTe_2$  using the WIEN2k and CASTEP codes to optimize their energy to the ground state. The optimized results were then compared with existing theoretical and experimental data for validation. The findings reveal that both  $KAlTe_2$  and  $KInTe_2$  exhibit both direct and indirect band gaps, depending on the chosen symmetry points during the calculations. The calculated band gaps for  $KAlTe_2$  and  $KInTe_2$  are found to be 1.68 eV and 0.931 eV, respectively. This dual band-gap behavior indicates that these materials have significant potential for applications in both thermoelectric and optical devices, where direct band gap semiconductors are particularly desirable for efficient energy conversion and light emission. Additionally, the study highlights that the bonding in these materials is characterized by a mixture of covalent and ionic interactions, contributing to their unique electronic properties. The combination of these features makes  $KAlTe_2$  and  $KInTe_2$  promising candidates for advanced material applications, particularly in fields where the manipulation of band structure and bonding characteristics is crucial for optimizing device performance. This work provides valuable insights into the fundamental properties of these materials and paves the way for further exploration in practical applications.

**Keywords:** bonding nature; structural; bandgap; DFT; WIEN2k; CASTEP

## 1. Introduction

The emergence of thin nano-atomic layers in 2D semiconductor materials has revolutionized the development of modern semiconductor devices, owing to their unique properties, such as high flexibility, tunable band gaps, and enhanced light-matter interactions. These characteristics make 2D materials ideal candidates for applications in next-generation electronic, optoelectronic, and photonic devices. With the increasing demand for new magnetic and thermoelectric devices, it has become crucial to accurately predict and evaluate the physical properties of semiconductors that can fulfill these requirements. Researchers are especially focused on non-toxic 2D semiconductors, synthesized from abundant elements, to ensure their environmental sustainability and efficiency. Materials like  $KAlTe_2$  and  $KInTe_2$ , which belong to the A-B-X<sub>2</sub> family of compounds, are of significant interest due to their promising properties for use in optoelectronics, photovoltaics, and nonlinear optics [1–3]. The A-B-X<sub>2</sub> structure consists of an alkali metal (A), a group III element (B), and a chalcogen (X), forming a stable and versatile framework. In  $KAlTe_2$  and  $KInTe_2$ , potassium (K) serves as the alkali metal with a valency of +1, aluminum (Al) or indium (In) have a valency of +3, and tellurium (Te) is a

chalcogen with a valency of -2. This stoichiometry ensures stability and is integral to the materials' desirable properties. Both  $\text{KAlTe}_2$  and  $\text{KInTe}_2$  crystallize in a tetragonal structure, where the lattice constants  $a$  and  $b$  are equal, and the  $c$ -axis differs, giving rise to unique electronic and structural characteristics. While earlier research has provided insights into the crystallography of these materials, some structural aspects, such as detailed bonding characteristics and thermodynamic behavior, remain underexplored. Previous studies have mainly focused on the atomic positions and bond lengths in single crystals of  $\text{KAlTe}_2$  and  $\text{KInTe}_2$ . Still, further investigation into the bonding and interaction of atoms is necessary to fully understand their behavior. Mulliken population analysis has revealed that the Aluminum-Tellurium (Al-Te) and Indium-Tellurium (In-Te) bonds are predominantly covalent, while the Potassium-Tellurium (K-Te) bond is ionic. This is consistent with the general trend observed in A-B-X<sub>2</sub> compounds, where the B-X bonds tend to be covalent, and the A-X bonds are ionic. These findings are aligned with experimental observations and provide a deeper understanding of the materials' atomic-level behavior. Given the intriguing properties of  $\text{KAlTe}_2$  and  $\text{KInTe}_2$ , there is a growing interest in exploring their thermoelectric and magnetic characteristics, especially at different temperatures, to unlock their potential in energy conversion and storage applications. Additionally, investigating their thermodynamic properties, which have yet to be fully explored, could further enhance the understanding of these materials and expand their applications in advanced technological devices [4–9].

## 2. Method of Calculations

Material properties can be investigated using both experimental and theoretical approaches. Experimentally, properties are often studied by analyzing wave functions derived from the Schrödinger Wave Equation. Theoretically, Density Functional Theory (DFT) provides a powerful framework for material analysis, grounded in the Kohn-Sham Equation. DFT-based tools play a crucial role in exploring various material properties, including electronic, structural, and mechanical characteristics. Among the DFT methods, the Full-Potential Linearized Augmented Plane Wave (FP-LAPW) approach, implemented in computational packages like WIEN2k and CASTEP, is widely used for analyzing complex materials such as  $\text{KAlTe}_2$  and  $\text{KInTe}_2$ . This method is particularly effective in providing accurate calculations of the electronic structure and bonding characteristics of materials. In structural studies, the exchange-correlation energy is commonly described using the Generalized Gradient Approximation (GGA), specifically the GGA-PBEsol functional, as formulated by Perdew et al. [10–14]. The GGA-PBEsol functional is well-regarded for its ability to provide reliable results for the structural properties of materials. When investigating the electronic properties, the band gap is a critical parameter. For conductors, semiconductors, insulators, and superconductors, the band gap is often calculated using standard GGA functionals. While GGA provides reasonable estimates of band gaps, it is known to underestimate them in certain materials, particularly semiconductors and insulators. This limitation has led to the development of more advanced functionals within the GGA framework, which aim to provide a more accurate representation of electronic structures across different types of materials. These advancements help overcome challenges in modeling and predicting material properties more effectively. Other DFT methods, such as the Local Density Approximation (LDA), meta-GGA, and hybrid functionals, are also used to calculate the mechanical properties of materials, each offering unique strengths in addressing the mechanical and electronic behaviors of complex systems [15–17].

## 3. Results and Discussion

In this section we are investigating the structural, bandgap and Bonding properties of ternary telluride.

### 3.1. Structural Properties:

The structural features of tetragonal materials were investigated using the full-potential Linearized Augmented Plane Wave (FP-LAPW) method, a well-established technique in density functional theory (DFT). This approach employed the Generalized Gradient Approximation (GGA) to analyze the DFT volume of unit cell structures and examine the chemical compositions. Specifically, the ternary tellurides  $\text{KAlTe}_2$  and  $\text{KInTe}_2$  were studied, both of which crystallize in the tetragonal space group  $I4/mcm$  (No. 140). The unit cell arrangements of these materials are shown in the accompanying Figures 3.1.(1)(2). In these structures, the Wyckoff positions of the atoms are defined as follows: Te atoms occupy the 8h sites with coordinates (0.1645, 0.6645, 0), K atoms are situated at the 4a sites with coordinates (0, 0, 0.25), and the atoms (Al or In) are located at the 4b sites with coordinates (0, 0.50, 0.25). These arrangements form distinctive structural units. The  $\text{XTe}_4$  tetrahedral units consist of Al or In cations surrounded by four Te atoms in a slightly distorted tetrahedral geometry [1,18–21]. Meanwhile, the K cations are positioned at the center of quadratic antiprisms composed of eight Te anions, resulting in  $\text{KTe}_8$  octahedral units. These unique geometries are illustrated in Figures 3.1.2(a) and 2(b). The coordination behavior of these structures provides further insight into their crystallography. In a body-centered cubic (BCC) lattice, the coordination number (CN) is 8, as each atom has eight nearest neighbors. In contrast, the face-centered cubic (FCC) lattice has a CN of 12 due to its denser packing and 12 nearest neighbors. The body-centered tetragonal (BCT) structure emerges as a transitional phase when the cubic lattice is distorted in one direction. This intermediate structure bridges the characteristics of BCC and FCC lattices, theoretically resulting in a coordination number that lies between 8 and 12, depending on the degree of distortion and specific atomic arrangement. The structural complexity of  $\text{KAlTe}_2$  and  $\text{KInTe}_2$ , including their tetrahedral and octahedral configurations, reflects the interplay of symmetry, bonding, and atomic packing within the tetragonal system. These features not only define their unique electronic and structural properties but also highlight the versatility of the FP-LAPW method and GGA in exploring the detailed crystallographic and chemical characteristics of advanced materials.

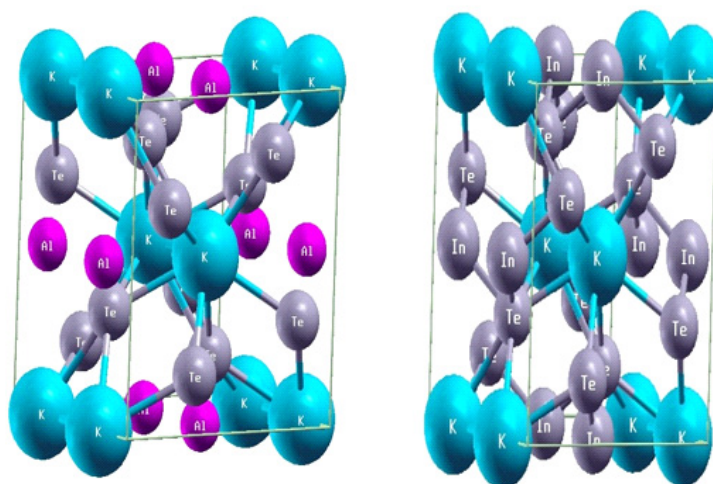
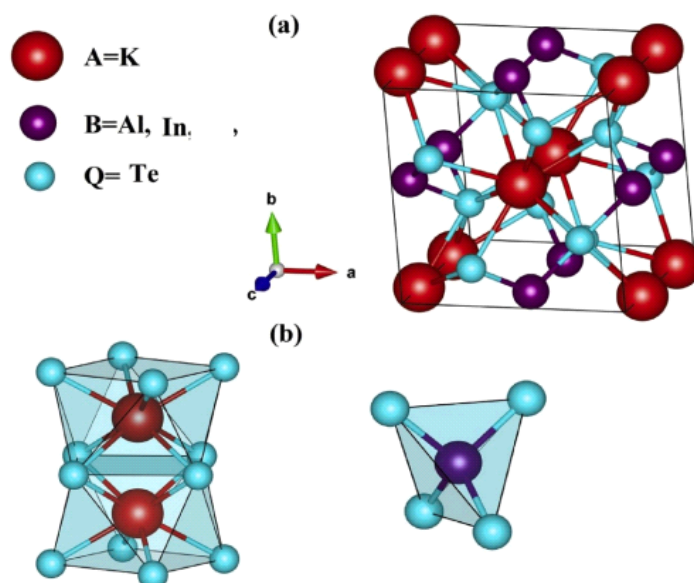


Figure 3.1.1. unit cells of investigated materials using WIEN2k Code.



**Figure 3.1.2.** unit cells of investigated materials using CASTEP Code.

### 3.2. Optimization Plots:

Optimization plays a pivotal role in theoretical calculations as it establishes a material's ground-state structural properties, which are essential for understanding its stability and behavior. This process involves minimizing the energy of a compound to its lowest possible level, thereby identifying the most stable configuration. During optimization, various structural files are generated, each representing a potential configuration of the material. These configurations are evaluated iteratively until the ground-state energy is achieved. For materials like  $\text{KAlTe}_2$  and  $\text{KInTe}_2$ , optimization is conducted using the WIEN2k package, which employs the percent  $c/a$  ratio from the initial structural file to refine the lattice parameters as shown in Figure 3.2.1. By systematically adjusting the  $c/a$  ratio, the method pinpoints the structural configuration with the minimum energy. The energy variation as a function of the percent  $c/a$  ratio reveals key insights into the relative stability of the compounds. Specifically, the optimization data show that in the tetragonal structure,  $\text{KAlTe}_2$  is more stable than  $\text{KInTe}_2$ , as evidenced by its lower ground-state energy. The structural parameters derived from this process are presented in the accompanying existed values, which highlights their accuracy by comparing them to previous experimental and theoretical findings [22–24]. The comparison demonstrates strong agreement, validating the reliability of the optimization methodology. These results not only affirm the stability of  $\text{KAlTe}_2$  in the tetragonal structure but also underscore the broader significance of optimization in theoretical studies. By providing a detailed understanding of structural properties, optimization serves as a foundation for further investigations into the electronic, optical, and mechanical behavior of materials. This iterative and precise approach is indispensable for accurately modeling and predicting the properties of advanced materials, ensuring consistency with experimental and theoretical benchmarks.

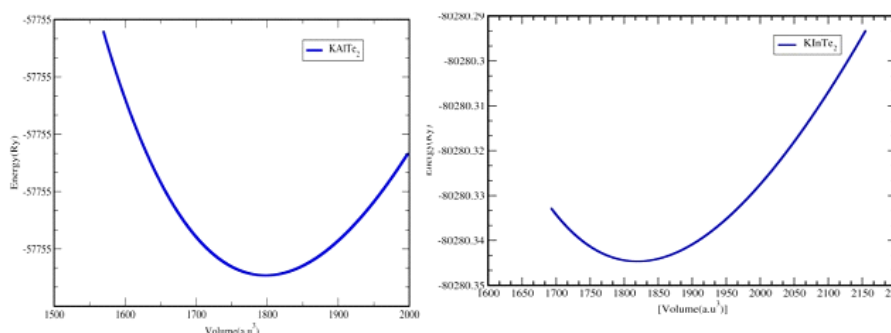


**Figure 3.2.1.** Optimization Plots Draw through WIEN2k Code.

### 3.3. Band Structure:

Tellurides are naturally intrinsic semiconductors, but doping with potassium and aluminum/indium transforms them into extrinsic semiconductors with tailored electronic properties. The band gap, a critical parameter for semiconductors, can be roughly estimated from density of states (DOS) plots. However, DOS analysis alone does not reveal whether the band gap is direct or indirect. Determining the band gap's nature requires examining the band structure at various symmetry points. If the energy states form curves at different symmetry points, the band gap is indirect. Conversely, a direct band gap is identified when the conduction band minima and valence band maxima align at the same symmetry point. Figure 3.3.(1) and (2) demonstrates the band structures of  $\text{KAlTe}_2$  and  $\text{KInTe}_2$ , calculated using the Generalized Gradient Approximation (GGA) method within the DFT framework. The analysis reveals that both materials are direct band gap semiconductors, as the conduction band minima and valence band maxima are aligned at the  $\Gamma$  symmetry point. Further confirms these results, showing the Fermi energy level set at 0.0 eV. For  $\text{KAlTe}_2$ , the conduction band minima and valence band maxima are located within the first Brillouin zone, affirming its direct band gap nature. Similarly,  $\text{KInTe}_2$  exhibits direct band gap characteristics, supported by contributions from critical symmetry points like R,  $\Gamma$ , X, and M. The calculated band gaps for  $\text{KAlTe}_2$  and  $\text{KInTe}_2$  using the GGA approach are 1.68 eV and 0.931 eV, respectively [3,25–27]. These values align with earlier studies based on DFT. When recalculated using the HSE06 functional, the band gaps were refined to 2.178 eV for  $\text{KAlTe}_2$  and 1.858 eV for  $\text{KInTe}_2$ , providing further accuracy. The agreement between theoretical predictions and experimental findings underscores the reliability of the computational models used. The semiconducting nature of  $\text{KAlTe}_2$  and  $\text{KInTe}_2$ , combined with their direct band gap properties, makes them highly suitable for various optoelectronic applications. These include photovoltaic devices, light-emitting diodes (LEDs), and other technologies requiring materials with high transparency or controlled absorption. Their band gap values indicate potential for use in devices operating within specific energy ranges, ensuring efficient performance and broad applicability. These findings emphasize the potential of doped tellurides in advancing next-generation electronic and optoelectronic technologies.

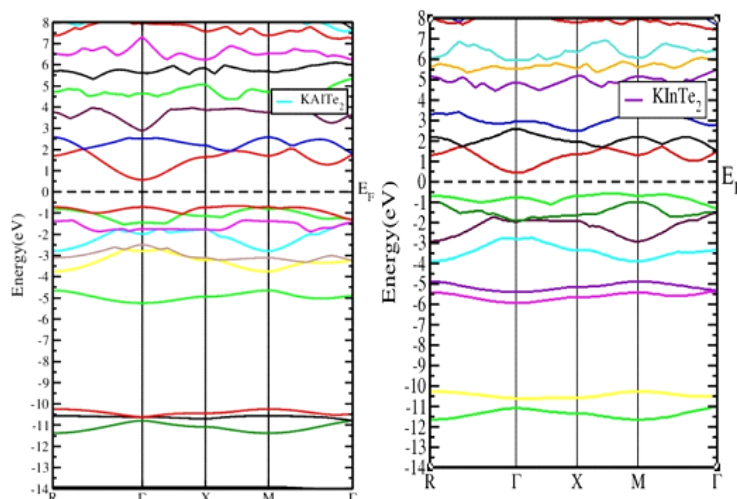


Figure 3.3.1. Band gaps of concern materials using WIEN2k Code.

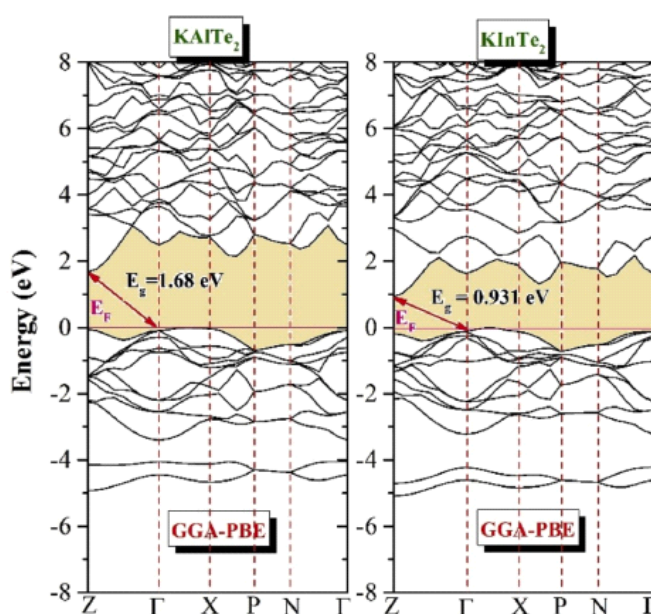
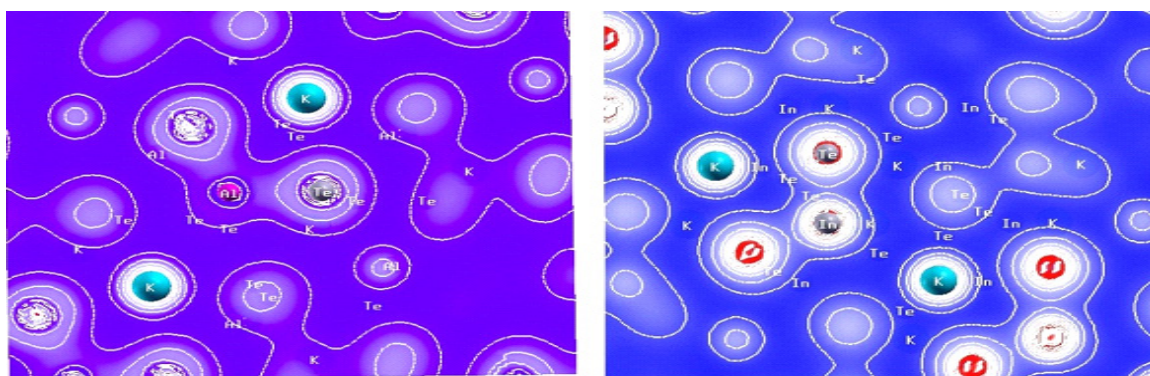


Figure 3.3.2. Band gaps of concern materials using CASTEP Code.

#### 3.4. Bonding Nature/Electron charge density:

The electron density plots provided in the following Figure 3.4 offer valuable insights into the bonding nature and charge transfer within the crystal structures of  $\text{KAlTe}_2$  and  $\text{KInTe}_2$ . These plots visually represent the distribution of electron density across the material, helping to elucidate the types of bonds between the various ions and providing a clearer understanding of the material's overall electronic characteristics. In  $\text{KAlTe}_2$ , the electron density around the potassium ion is nearly spherical, which suggests that the potassium bonds are more ionic in nature compared to covalent. This indicates that potassium primarily forms ionic interactions with other atoms in the structure. On the other hand, the electron density reveals a strong covalent bond between aluminum and tellurium atoms. The electron cloud distribution around aluminum and tellurium shows a more directional bonding nature, characteristic of covalent bonds. This trend is similarly observed in  $\text{KInTe}_2$ , where indium and tellurium also exhibit a strong covalent bond. However, the potassium-tellurium bond in  $\text{KInTe}_2$ , like in  $\text{KAlTe}_2$ , remains predominantly ionic. This ionic-covalent bonding pattern aligns

with what has been observed in other A-B-X<sub>2</sub> structures, where A represents an alkali metal and B and X are other elements. In these structures, the B-X bonds (such as aluminum-tellurium or indium-tellurium) tend to be primarily covalent, while the A-X bonds (such as potassium-tellurium) are predominantly ionic. These bonding characteristics are consistent with experimental observations and theoretical predictions in similar materials [1,3,28]. The unique bonding nature in KAlTe<sub>2</sub> and KInTe<sub>2</sub> plays a crucial role in their electronic properties. The ionic and covalent interactions contribute to the material's overall stability and electronic behavior, making them suitable candidates for various applications. Their distinctive charge transfer properties and bonding types make these materials particularly important for use in photovoltaic devices, optoelectronic applications, and nonlinear optical devices. As the demand for advanced materials in these technologies grows, KAlTe<sub>2</sub> and KInTe<sub>2</sub> are emerging as promising candidates due to their unique structural and electronic characteristics.



**Figure 3.4.** Bonding Nature of studied Materials Using WIEN2k Code.

### 3.5. Mechanical Nature:

The mechanical properties of the investigated materials, KAlTe<sub>2</sub> and KInTe<sub>2</sub>, have been rigorously analyzed through advanced computational methods, with the results systematically presented in Tables 3.1 and 3.2. These analyses were performed using the Generalized Gradient Approximation (GGA) framework within the renowned WIEN2k and CASTEP computational codes. Both methods are widely acknowledged for their precision in simulating the electronic and structural properties of complex materials, making them suitable for accurate mechanical property calculations. The study focuses on key mechanical parameters, including elastic constants, bulk modulus, shear modulus, Young's modulus, and Poisson's ratio. These parameters are essential for understanding the materials' structural rigidity, mechanical stability, and their potential for practical applications in various technological fields [29,30]. The application of the GGA approach ensures improved accuracy in the computations by incorporating corrections to the exchange-correlation energy, providing a more realistic representation of the materials' mechanical responses under various conditions. This approach also offers a good balance between computational efficiency and the precision required for the analysis of mechanical properties. In addition, the use of WIEN2k and CASTEP codes allows for a detailed exploration of the intricate relationship between the crystallographic structure and the mechanical properties of these materials. DFT calculations are typically performed at various temperature values to assess the temperature dependence of the mechanical properties. Several DFT methods, including Local Density Approximation (LDA), meta-GGA, hybrid functionals, and Full-Potential Linearized Augmented Plane Wave (FP-LAPW), are employed to calculate the mechanical properties of materials. While GGA is widely used due to its balance between accuracy and computational cost, the FP-LAPW method provides higher precision, particularly for more complex systems, by treating both core and valence electrons separately. The findings from this study contribute to a deeper understanding of KAlTe<sub>2</sub> and KInTe<sub>2</sub>, supporting their potential for innovative technological applications.

Table 3.1. of the material  $\text{KAlTe}_2$  using two mentioned codes.

Elastic Constants	$\text{KAlTe}_2$
<b>Bulk Modulus, Voigt</b>	18 GPa
<b>Bulk Modulus, Reuss</b>	17 GPa
<b>Bulk Modulus, Voigt-Reuss-Hill</b>	17 GPa
<b>Shear Modulus, Voigt</b>	12 GPa
<b>Shear Modulus, Reuss</b>	10 GPa
<b>Shear Modulus, Voigt-Reuss-Hill</b>	11 GPa
<b>Poisson's Ratio</b>	0.24
<b>Universal Anisotropy</b>	0.68

Table 3.2. of the material  $\text{KInTe}_2$  using two mentioned codes.

Elastic Constants	$\text{KInTe}_2$
<b>Bulk Modulus, Voigt</b>	15 GPa
<b>Bulk Modulus, Reuss</b>	15 GPa
<b>Bulk Modulus, Voigt-Reuss-Hill</b>	15 GPa
<b>Shear Modulus, Voigt</b>	10 GPa
<b>Shear Modulus, Reuss</b>	9 GPa
<b>Shear Modulus, Voigt-Reuss-Hill</b>	9 GPa
<b>Poisson's Ratio</b>	0.24
<b>Universal Anisotropy</b>	0.70

## Conclusion

In summary, the physical properties of  $\text{KAlTe}_2$  and  $\text{KInTe}_2$ , including their structural, band gap, and bonding characteristics, were analyzed using first-principles methods. The computed crystal structure properties are in excellent agreement with existing experimental data, confirming the

tetragonal crystal structure of both materials. The analysis reveals that these materials exhibit strong covalent bonding between aluminum/indium and tellurium, while the potassium-tellurium bond is predominantly ionic, highlighting their anisotropic and stable nature. Density functional theory (DFT) calculations also predict that these materials are ductile, indicating mechanical flexibility. The band gap analysis, based on the Generalized Gradient Approximation (GGA) technique, reveals that  $\text{KAlTe}_2$  is a direct band gap semiconductor with a band gap of 1.68 eV, while  $\text{KInTe}_2$  is an indirect band gap semiconductor with a band gap of 0.931 eV. The findings suggest that replacing aluminum with indium in  $\text{KAlTe}_2$  reduces the band gap numerically, making  $\text{KInTe}_2$  more suited for applications requiring different band gap properties. These results confirm the significant potential of  $\text{KAlTe}_2$  and  $\text{KInTe}_2$  in material science, particularly for optoelectronic applications such as photovoltaic devices, light-emitting diodes, and other technologies requiring specific electronic properties. The comparison with previous experimental and theoretical data demonstrates the reliability of the first-principles approach in predicting the behavior of these materials.

**Funding:** This research received no specific grant from any funding agency in the public, commercial, or not-for-profit sectors.

## References

1. M Bouchenafa, A Benmakhlouf, M Sidoumou, A Bouhemadou, S Maabed, M Halit, and Y Al-Douri. Theoretical investigation of the structural, elastic, electronic, and optical properties of the ternary tetragonal tellurides  $\text{KBTe}_2$  (B= Al, In). *Materials Science in Semiconductor Processing*, 2020, **114**, 105085-105088.
2. A Benmakhlouf, A Bentabet, A Bouhemadou, S Maabed, R Khenata, and S Bin-Omran. Structural, elastic, electronic and optical properties of  $\text{KAlQ}_2$  (Q= Se,Te): A DFT study. *Solid State Sciences*, 2015, **48**, 72-81.
3. Ullah, Z., Amir, M., Bazilla, A., Ullah, S., Shahzad, U., Ullah, N., ... & Gul, S. (2024). Electronic, Thermoelectric and Magnetic properties of Ternary Telluride  $\text{KAlTe}_2$  and  $\text{KInTe}_2$  from Theoretical Perspective. *Next Research*, 100077.
4. G Belgoumri, A Bentabet, R Khenata, Y Bouhadda, A Benmakhlouf, D.P Rai, S Bounab. Insight into the structural, electronic and elastic properties of  $\text{AlInQ}_2$  (A: K, Rb and Q: S, Se, Te) layered structures from first-principles calculations. *Chinese Journal of Physics*, 2018, **56**(3), 1074-1088.
5. A Benmakhlouf. Structural, elastic, electronic and optical properties of  $\text{KAlQ}_2$  (Q= Se, Te): a DFT study, *Solid State Sci*, 2015, **48**, 72–81.
6. K kish Feng. Synthesis structure, physical properties, and electronic structure of  $\text{KGaSe}_2$ , *Solid State Sci*, 2012, **14** (8), 1152–1156.
7. J Kim, T Hughbanks. Synthesis and structures of ternary chalcogenides of aluminum and gallium with stacking faults:  $\text{KMQ}_2$  (M= Al, Ga; Q= Se, Te). *Journal of Solid-State Chemistry*, 2000, **149**(2), 242-251.
8. C W Witt, W B Shires, W C Tan, J W Jankowski, and J C Pickard. Random Structure Searching with Orbital-Free Density Functional Theory. *The Journal of Physical Chemistry A*, 2021, **125**(7), 1650-1660.
9. Trani, F., Ninno, D., Cantele, G., Iadonisi, G., Hameeuw, K., Degoli, E., & Ossicini, S. (2006). Screening in semiconductor nanocrystals: Ab initio results and Thomas-Fermi theory. *Physical Review B—Condensed Matter and Materials Physics*, 73(24), 245430.
10. Xie, Q. X., Wu, J., & Zhao, Y. (2021). Accurate correlation energy functional for uniform electron gas from an interpolation ansatz without fitting parameters. *Physical Review B*, 103(4), 045130..
11. Claeys, C., Hsu, P. C., Mols, Y., Han, H., Bender, H., Seidel, F., ... & Simoen, E. (2020). Electrical Activity of Extended Defects in Relaxed  $\text{In}_x\text{Ga}_{1-x}$  Hetero-Epitaxial Layers. *ECS Journal of Solid State Science and Technology*, 9(3), 033001.
12. Ikeda, A., Koibuchi, S., Kitao, S., Oudah, M., Yonezawa, S., Seto, M., & Maeno, Y. (2019). Negative ionic states of tin in the oxide superconductor  $\text{Sr}_{3-x}\text{SnO}$  revealed by Mössbauer spectroscopy. *Physical Review B*, 100(24), 245145.
13. Tran, F. (2018). WIEN2k: An Augmented Plane Wave Plus Local Orbitals Program for Calculating Crystal Properties.

14. Madsen, G.K.H., & Singh, D.J. BoltzTraP. A code for calculating band-structure dependent quantities. *Comput. Phys. Commun.*, 2006, 175(1), 67-71.
15. Wu, C. S., Lee, P. Y., & Chai, J. D. (2016). Electronic properties of cyclacenes from TAO-DFT. *Scientific reports*, 6(1), 37249.
16. Engel, J., Francis, S., & Roldan, A. (2019). The influence of support materials on the structural and electronic properties of gold nanoparticles—a DFT study. *Physical Chemistry Chemical Physics*, 21(35), 19011-19025.
17. Feng, S., Wang, N., Li, M., Xiao, H., Liu, Z., Zu, X., & Qiao, L. (2021). The thermal and electrical transport properties of layered LaCuOSe under high pressure. *Journal of Alloys and Compounds*, 861, 157984.
18. Wiebeler, H. (2020). A linear scaling DFT-Method and high-throughput calculations for p-type transparent semiconductors (Doctoral dissertation, Universitätsbibliothek).
19. Schwarz, K., & Blaha, P. (2003). Solid state calculations using WIEN2k. *Computational Materials Science*, 28(2), 259-273.
20. Schwarz, K. (2003). DFT calculations of solids with LAPW and WIEN2k. *Journal of Solid State Chemistry*, 176(2), 319-328.
21. Labrim, H., Jabar, A., Laanab, L., Jaber, B., Bahmad, L., Selmani, Y., & Benyoussef, S. (2023). Optoelectronic and thermoelectric properties of the perovskites: NaSnX<sub>3</sub> (X= Br or I)—a DFT study. *Journal of Inorganic and Organometallic Polymers and Materials*, 33(10), 3049-3059.
22. Selmani, Y., Labrim, H., Mouatassime, M., & Bahmad, L. (2022). Structural, optoelectronic and thermoelectric properties of Cs-based fluoroperovskites CsMF<sub>3</sub> (M= Ge, Sn or Pb). *Materials Science in Semiconductor Processing*, 152, 107053.
23. Bouhmaidi, S., Marjaoui, A., Talbi, A., Zanouni, M., Nouneh, K., & Setti, L. (2022). A DFT study of electronic, optical and thermoelectric properties of Ge-halide perovskites CsGeX<sub>3</sub> (X= F, Cl and Br). *Computational Condensed Matter*, 31, e00663.
24. Prihadi, H. L., Zen, F. P., Ariwahjoedi, S., & Dwiputra, D. (2023). Replica trick calculation for entanglement entropy of static black hole spacetimes. *International Journal of Geometric Methods in Modern Physics*, 20(08), 2350132.
25. H K G Madsen, and J D Singh. BoltzTraP. A code for calculating band-structure dependent quantities. *Comput. Phys. Commun.*, 2006, 175(1), 67-71.
26. Kaur, T., & Sinha, M. M. (2021). Probing thermoelectric properties of high potential Ca<sub>3</sub>PbO: An Ab Initio Study. In *IOP Conference Series: Materials Science and Engineering* (Vol. 1033, No. 1, p. 012080). IOP Publishing.
27. Mahmood, Q., Hassan, M., Ahmad, S. H. A., Bhamu, K. C., Mahmood, A., & Ramay, S. M. (2019). Study of electronic, magnetic and thermoelectric properties of AV<sub>2</sub>O<sub>4</sub> (A= Zn, Cd, Hg) by using DFT approach. *Journal of Physics and Chemistry of Solids*, 128, 283-290.
28. S Feng, N Wang, M Li, H Xiao, Z Liu, X Zu, and L Qiao. The thermal and electrical transport properties of layered LaCuOSe under high pressure. *Journal of Alloys and Materials*, 2021, 861, 157984-157989.
29. Ribeiro, R. A., Andres, J., Longo, E., & Lazaro, S. R. (2018). Magnetism and multiferroic properties at MnTiO<sub>3</sub> surfaces: A DFT study. *Applied Surface Science*, 452, 463-472.
30. N Benmekideche, A Bentabet, Y Bouhadda, D Boubatra, G Belgoumri, and S Fetah, K Benyelloul. DFT study of structural, electronic and elastic properties of two polymorphs of monoclinic CsGaQ<sub>2</sub> (Q= S, Se). *Chinese Journal of Physics*, 2019, 56(3), 1345-1352.

**Disclaimer/Publisher's Note:** The statements, opinions and data contained in all publications are solely those of the individual author(s) and contributor(s) and not of MDPI and/or the editor(s). MDPI and/or the editor(s) disclaim responsibility for any injury to people or property resulting from any ideas, methods, instructions or products referred to in the content.